Research Square

Preprints are preliminary reports that have not undergone peer review.
They should not be considered conclusive, used to inform clinical practice,
or referenced by the media as validated information.

# Placental co-expression signatures associated with pre-eclampsia and antenatal blood pressure: a multi-cohort secondary transcriptomic analysis

**Qiang Li**
Yinchuan Maternal and Child Health Hospital Affiliated to Ningxia Medical University
**Weiqiang Ma**
Yinchuan Maternal and Child Health Hospital Affiliated to Ningxia Medical University
**Yongdong Zhao**
Yinchuan Maternal and Child Health Hospital Affiliated to Ningxia Medical University
**Yali Zhang**
Yinchuan Maternal and Child Health Hospital Affiliated to Ningxia Medical University
**Haoming Liu**
Yinchuan Maternal and Child Health Hospital Affiliated to Ningxia Medical University
**Mingjun Wang**
26802424@qq.com

Yinchuan Maternal and Child Health Hospital Affiliated to Ningxia Medical University

**Research Article**

**Keywords:**

**Posted Date:** November 27th, 2026

**DOI:** https://doi.org/10.21203/rs.3.rs-11359900/v1

**License:** This work is licensed under a Creative Commons Attribution 4.0 International License.
Read Full License

**Additional Declarations:** No competing interests reported.

**Title:Placental co-expression signatures associated with pre-eclampsia and antenatal blood pressure: a multi-cohort secondary transcriptomic analysis**

**Author names and affiliations：**

Qiang Li[1]*, Weiqiang Ma[1], Yongdong Zhao[1],Yali Zhang[1],Haoming Liu[1], Mingjun Wang[1]*

[1] Department of Anesthesiology, Yinchuan Maternal and Child Health Hospital Affiliated to Ningxia Medical University, Yinchuan, Ningxia 750001, China

***Corresponding author:**

Qiang Li and Mingjun Wang

Department of Anesthesiology and Perioperative Medicine

Yinchuan Maternal and Child Health Hospital Affiliated to Ningxia Medical University

Yinchuan, Ningxia 750001, China

Email: 137069969@qq.com(Qiang Li);26802424@qq.com(Mingjun Wang)

## Abstract

**Background:** Haemodynamic heterogeneity in pre-eclampsia is relevant to obstetric anaesthesia, but its relationship with placental transcriptomic patterns requires evaluation in the context of antenatal blood pressure and overlapping placental disorders. We aimed to identify placental co-expression modules associated with pre-eclampsia and examine their associations with maximum antenatal blood pressure.

**Methods:** We conducted a retrospective secondary analysis of 339 samples from four publicly available bulk placental transcriptomic cohorts. A weighted gene co-expression network was constructed using 157 discovery samples. Associations with maximum antenatal systolic and diastolic blood pressure were examined in the full cohort and among 80 women with pre-eclampsia, with adjustment for clinical variables and cell-lineage proxies. External cohorts were used to assess module preservation and fixed module scores. Single-cell reference and tissue-compartment data were used to describe expression localisation. Classification analyses were exploratory.

**Results:** The primary blue module comprised 543 genes. After adjustment for clinical variables and cell-lineage proxies, each standard-deviation increase in its eigengene was associated with a 7.02 mmHg higher maximum systolic blood pressure (95% confidence interval [CI] 2.64 – 11.41) and a 4.48 mmHg higher maximum diastolic blood pressure (95% CI 1.59 – 7.37) in the full cohort; both false discovery rates were 0.0338. Associations within the pre-eclampsia subgroup did not survive multiple-testing correction. Module preservation Zsummary values were 3.93, 26.35 and 33.37 across the three external cohorts. In the independent RNA-sequencing cohort, module scores were higher in both isolated pre-eclampsia and isolated fetal growth restriction than in controls; *MME, FLT1, ENG* and *PAPPA2* showed increased expression in pre-eclampsia. The fixed three-gene score distinguished pre-eclampsia from controls with an area under the curve of 0.986, but improved discrimination over *FLT1* alone was not established.

**Conclusions:** We identified a placental expression signature associated with maximum antenatal blood pressure in the discovery cohort and showing overlap between pre-eclampsia and fetal growth restriction. These findings identify candidate molecular features for future studies of haemodynamics in obstetric anaesthesia, but do not establish a blood pressure gradient within pre-eclampsia. Post-anaesthetic hypotension and vasopressor responses were not directly assessed.

**Keywords:** Pre-eclampsia; Placenta; Antenatal blood pressure; Co-expression network; Fetal growth restriction; Cell lineage; Obstetric anaesthesia

## Introduction

Pre-eclampsia (PE) can affect multiple maternal organs and the placenta, and its peripartum management must balance maternal safety with fetal wellbeing[1]. For women with PE undergoing caesarean delivery, anaesthetic management requires a balance between controlling severe hypertension, avoiding excessive blood pressure reductions after anaesthesia and maintaining organ perfusion[1, 2]. Direct haemodynamic observations in women with severe PE have shown that blood pressure changes after neuraxial anaesthesia and uterotonic administration do not necessarily parallel changes in cardiac output[3]. The disease biology associated with maternal blood pressure therefore warrants investigation in obstetric anaesthesia, although antenatal blood pressure and dynamic circulatory responses after anaesthesia represent distinct phenotypes.

The anaesthetic haemodynamic profile of PE cannot be characterised simply as an increased susceptibility to hypotension after spinal anaesthesia. A prospective comparative study found a lower incidence of post-spinal hypotension and lower ephedrine requirements in women with severe PE than in healthy women undergoing elective caesarean delivery[4]. A dose–response study also observed, under its study conditions, a lower effective phenylephrine dose for treating the first episode of post-spinal hypotension in women with severe PE[5]. In addition, hypertensive disorders of pregnancy accompanied by fetal growth restriction (FGR) may have distinct maternal haemodynamic profiles[6]. These observations highlight the need to

distinguish disease phenotypes and their heterogeneity rather than presupposing the direction of an association between placental abnormalities and post-anaesthetic hypotension.

The placenta provides an important biological link between PE and maternal vascular dysfunction. Clinical and experimental studies have implicated soluble fms-like tyrosine kinase 1 (sFLT1) and soluble endoglin (sENG) in antiangiogenic signalling and endothelial dysfunction[7, 8]. However, PE and FGR do not have identical placental molecular backgrounds. A prospective study found that, although both conditions could be preceded by an elevated maternal serum sFLT1-to-placental growth factor ratio, the associated placental protein changes differed[9]. Evaluation of placental expression signatures therefore requires a distinction between changes associated with maternal PE and abnormalities shared by multiple placental disorders. Gene-level *FLT1* or *ENG* expression cannot substitute for measurements of circulating soluble proteins or vascular function.

Previous placental transcriptomic studies have demonstrated molecular heterogeneity in PE and identified co-expression modules associated with maternal blood pressure in early-onset PE with and without FGR[10, 11]. Single-cell reference-based studies have also shown that differences in cellular composition can account for part of the PE-associated expression signal in bulk tissue[12]. It remains unclear whether PE-related modules are associated with antenatal blood pressure after accounting for disease status, gestational age, chronic hypertension and cell-lineage-related factors, and whether such associations can be observed within women with PE. Cross-cohort preservation of network structure and disease specificity also require separate evaluation.

We performed a secondary analysis of multiple public placental transcriptomic cohorts, focusing on PE-related co-expression modules and their associations with maximum antenatal systolic and diastolic blood pressure. We evaluated the robustness and disease context of these signals through adjustment for clinical variables and cell-lineage proxies, network stability and external preservation analyses, and comparisons among PE, FGR and their coexistence. Reference-based cellular

localisation and an existing classification score were used to support interpretation. The aim was to generate testable molecular hypotheses for future obstetric anaesthesia haemodynamic research, rather than to develop a model directly predicting post-anaesthetic hypotension.

## Methods

### Study design and data sources

We retrospectively analysed public human placental transcriptomic data. GSE75010 was the discovery cohort; GSE25906 and GSE10588 provided supportive replication; and GSE114691 provided new external RNA-sequencing evaluation across controls, isolated PE, isolated FGR and PE with FGR[10, 13–17]. GSE114691 primarily involved early-onset disease and preterm comparisons. GSE182381 supplied a healthy term single-cell reference, and GSE93839 supplied microdissected tissue-compartment data[12, 18–20]. Dataset roles and observational units are summarised in Table 1 and Fig. 1. Additional file 1 combines supplementary methods, Figures S1–S4 and five focused tables; source results and scripts remain in the separate source-results and code archive.

Disease groups followed the clinical annotations in the source data, without diagnostic readjudication. The non-PE group in the discovery cohort included 24 women with chronic hypertension. The primary blood pressure outcomes were the maximum antenatal systolic blood pressure (SBP) and diastolic blood pressure (DBP) recorded in the source data; the two maxima did not necessarily originate from the same measurement. Data on anaesthetic exposure, intraoperative blood pressure trajectories and vasopressor responses were unavailable. Cells and tissue compartments were not counted as additional independent patients. The sample size was determined by the available eligible public samples; no prospective sample size calculation was performed.

Discovery module definitions and classification coefficients were fixed before importing GSE114691 expression data. Previously explored GSE25906 and GSE10588 were supportive replication cohorts, rather than untouched validation

datasets.

**Expression data processing and cross-cohort comparisons**

Each microarray cohort was processed separately; intensity values from different platforms were neither pooled nor subjected to cross-cohort batch correction. Platform annotations were used to map probes to gene symbols, and unannotated probes and probes with ambiguous mappings were removed. For genes represented by multiple probes, the probe with the largest interquartile range was retained, without using disease labels. GSE10588 was $\log^2$-transformed after applying a lower bound of $10^{-6}$; the other matrices retained their source expression scales. Data quality was characterised using principal component analysis and expression-completeness checks.

Supportive microarray analyses standardised expression by within-cohort sample SD and estimated PE differences using ordinary least squares: GSE75010 adjusted for gestational age, fetal sex and chronic hypertension; GSE25906 additionally used its recorded batch instead of chronic hypertension; GSE10588 was unadjusted. Conventional residual variances and t-tests were used. Shared-gene effects were pooled using inverse-variance random-effects models with DerSimonian–Laird variance, normal-approximation CIs, Cochran's Q and $I^2$[21].This analysis reanalysed sample-level data and was not a systematic review.

GSE114691 public transcript counts were matched to specimen descriptions and aggregated by gene symbol using GRCh37/GENCODE v19 after removing ENST version suffixes; raw reads were not realigned. All 79 samples were retained. edgeR filterByExpr, recalculated library sizes and TMM normalisation preceded log-CPM scoring (prior count 2) and limma–voom differential expression with robust empirical Bayes moderation[22–25]. A four-group model without an intercept tested PE, FGR and PE with FGR versus controls, PE versus FGR, and PE with FGR versus PE. Each contrast was corrected across 26,044 retained genes. Individual-level clinical covariates were unavailable; unmapped candidates were not evaluable.

**Co-expression network, module stability and external preservation**

A signed network was constructed using weighted gene co-expression network

analysis (WGCNA) among the 5,000 genes with the highest variance in the discovery cohort[26]. Gene selection did not use disease labels; samples and selected genes passed goodSamplesGenes checks. Soft-thresholding powers from 1 to 20 were evaluated, and the first power meeting a signed scale-free topology fit $R^2 \geqslant 0.80$ with a negative fitted slope was selected. Pearson correlations, signed adjacency and signed topological overlap were used. The blockwiseModules parameters were deepSplit = 2, minimum module size = 40, merge cut height = 0.25 and maximum block size = 6000. Grey denoted unassigned genes.

Eigengenes were oriented to mean module expression and standardised by discovery SD. The assigned module most strongly correlated with PE in absolute terms was primary; kME was gene–eigengene correlation. With genes and parameters fixed, 30 networks were reconstructed in 80% subsamples (125 participants), comparing each reference module with its best non-grey match by Jaccard overlap. Sensitivity analyses used powers 15 and 17 and biweight midcorrelation (maxPOutliers = 0.1).

External modulePreservation used shared genes, 200 permutations, a signed network, maximum module size 5000 and maximum gold-module size 500 [27]. Zsummary, medianRank and coverage assessed network structure, separately from disease specificity or expression differences.

**Cell-lineage proxy measures**

The 40,494 reference cells in GSE182381 were normalised to counts per 10000 (CP10K) over the supplied gene set. The 27 annotated clusters were grouped into seven major lineages: cytotrophoblast, syncytiotrophoblast, extravillous trophoblast, stromal, endothelial, immune and erythroid[12]. Among genes shared by the reference and discovery expression data, markers were required to have a within-lineage detection rate $\geqslant$ 15%, mean normalised expression $\geqslant$ 0.5 and positive specificity. Specificity was defined as $\log^2$[(mean expression in the target lineage + 0.1)/(maximum mean expression among other lineages + 0.1)]. Up to 50 markers with the highest specificity were retained per lineage.

Marker construction excluded 14 previously specified candidates (listed in

Additional file 1). Lineage scores were mean within-sample marker percentile ranks. Principal components of standardised scores explaining ⩾ 95% cumulative variance yielded six components. Excluding all 543 primary-module genes yielded seven components; both marker sets contained 342 genes (Supplementary methods). These were reference-derived proxies, not calibrated cell proportions.

**Blood pressure associations and sensitivity analyses**

Ordinary least squares models were fitted for the 13 assigned modules, using maximum antenatal SBP and DBP as continuous outcomes, separately in all 157 discovery participants and in the 80 women with PE. M1 adjusted for gestational age, fetal sex and chronic hypertension, with additional adjustment for PE status in the full cohort. M2 added the six primary lineage components to M1. M3 added the seven components obtained after excluding module genes to M1. Unadjusted models were also provided. Effects were expressed as blood pressure differences (mmHg) per one discovery-cohort SD increase in the module eigengene. Heteroscedasticity-robust HC3 standard errors and the t-distribution were used to construct 95% confidence intervals (CIs)[28].

M2 sensitivity analyses separately added IUGR, replaced linear gestational age with a cubic B-spline (3 degrees of freedom), added maternal age and caesarean delivery, or restricted gestational age to 28 – 36 weeks. IUGR and delivery mode were sensitivity variables rather than assumed baseline confounders. Constant covariates were omitted; complete cases were analysed without imputation, reporting sample sizes and module VIFs. PE expression differences used M1–M3; module–lineage associations used Spearman correlations.

**Fixed module scores and localisation of candidate-gene expression**

Within each cohort, the fixed module score was the mean of the z-scores of measurable member genes, multiplied by the sign of their discovery-cohort kME. Standardisation used the full cohort and the sample SD (denominator n − 1). Module membership and direction were not re-estimated using external disease labels. Missing genes were omitted from score calculation, and coverage was reported. Welch's t-tests were used for between-group comparisons, with mean differences and

95% CIs based on Satterthwaite degrees of freedom. Microarray cohorts were compared by PE versus non-PE status, and GSE114691 was evaluated using the five disease contrasts described above. Because standardisation was performed within each cohort, scores were cohort-dependent, and their units were not assumed to be directly comparable across cohorts.

Ten previously identified candidates were highlighted (listed in Additional file 1). Reference localisation used normalised means and detection rates, without treating individual cells as independent patients. Existing PE–control comparisons in invasive, endovascular and syncytial trophoblast compartments retained within-compartment genome-wide correction; repeated donor compartments were not pooled for new patient-level tests.

**Functional enrichment and association networks**

Over-representation analyses used archived GO Biological Process 2025, Reactome Pathways 2024 and KEGG 2021 Human gene sets, with all 5000 network genes, including unassigned genes, as the background. One-sided Fisher's exact tests were applied to terms containing 10–500 background genes; terms with no overlapping genes were retained in the multiple-testing family. Within-module and across-module false discovery rates (FDRs) were reported, with within-module correction serving as the primary basis for interpreting the primary module. Previously retrieved high-confidence STRING functional associations were used to describe connections among candidates, rather than proof of direct physical interactions[29].

**Exploratory classification model and external evaluation**

The earlier classification pipeline started from 1,476 measured genes in an annotation-defined vascular-related gene set, without preselection based on the current blue module or full-cohort differential expression results. Using scikit-learn, five-fold stratified outer cross-validation was repeated three times, giving 15 evaluations[30]. Within each outer training set, three-fold stratified inner cross-validation selected the number of features (25 or 75) and the inverse regularisation strength C (0.05, 0.2 or 1) according to the area under the receiver operating characteristic (ROC) curve (AUC). StandardScaler, univariate

analysis-of-variance feature selection and L1-regularised logistic regression were fitted within the pipeline, using balanced class weights and the liblinear solver. Mean outer AUC, descriptive SD and selection frequencies were used to evaluate the overall pipeline.

The fixed ranking score was $0.7871769602 \times z(\text{FLT1}) - 0.1556272653 \times z(\text{ELMO1}) + 0.0827561010 \times z(\text{MME})$. External standardisation used full-cohort population SD (n); coefficients were not refitted, making evaluation cohort-adaptive rather than directly applicable to an individual patient. Microarrays tested PE versus non-PE; GSE114691 tested PE, PE with FGR and FGR versus controls, plus PE versus FGR. AUC CIs used 2000 class-stratified bootstrap resamples. A post hoc FLT1-only comparison used paired resampling. Calibration, decision utility and anaesthetic outcomes were not evaluated.

**Statistical reporting and reproducibility**

Tests were two-sided except one-sided Fisher enrichment tests. Benjamini–Hochberg FDR $< 0.05$ defined significance[31]. Correction families were 26 blood-pressure tests per model/population; 91 module–trait tests; 14 archived selection eigengenes including grey (before displaying 13 assigned modules); separate 13-module and 14-gene PE-expression families per model; and all module-score comparisons per cohort. RNA-sequencing and supportive microarrays used their genome-wide families. CIs were nominal. Correction-family definitions appear in Additional file 1; complete results are retained in Additional file 2.

Analyses used R and Python; archived versions, seeds and environments are detailed in Additional file 1 and the source-results and code archive.

**Results**

**Study cohorts and data quality**

Four bulk datasets contributed 339 samples: GSE75010, 80 PE/77 non-PE; GSE25906, 23 PE/37 controls; GSE10588, 17 PE/26 controls; and GSE114691, 21 controls/20 PE/18 FGR/20 PE with FGR (Fig. 1A, B; Table 1). The first two external microarrays were supportive replication cohorts. The 40494 reference cells and 23 microdissected compartment samples were analysed separately (Fig. 1F; Fig. S4C).

All 157 discovery samples passed expression-completeness checks and had records for gestational age, fetal sex, chronic hypertension status, and maximum antenatal SBP and DBP. Maternal age was missing for two participants. Median gestational age was 32.29 weeks (interquartile range [IQR] 30.00 – 36.07) in the PE group and 35.86 weeks (IQR 30.57 – 38.71) in the non-PE group (Fig. 1E). The non-PE comparison group included 24 women with chronic hypertension and therefore was not composed exclusively of normotensive pregnancies.

In GSE114691, 95.97% of the public transcript counts were successfully mapped to gene symbols, and 26,044 genes were retained for differential expression analysis after expression filtering. Unsupervised principal component analysis showed disease-related expression variation, but the groups overlapped and were not completely separated (Fig. 1C, D; Additional file 1: Fig. S1A, B). Library counts, numbers of detected genes and clinical-variable completeness are shown in Additional file 1: Fig. S1C – F.

**PE-related co-expression modules and their stability**

WGCNA of the 5000 most variable genes in the discovery cohort identified 13 assigned modules containing 104 – 770 genes each; 1,605 genes remained unassigned. A soft-thresholding power of 16 was the first to satisfy the prespecified signed scale-free topology criterion, with $R^2 = 0.846$ and mean connectivity = 6.26 (Fig. 2A–D; Additional file 1: Table S1). The blue module, comprising 543 genes, had the strongest absolute correlation with PE status (r = 0.608). Its eigengene was also positively correlated with maximum antenatal SBP (r = 0.655), DBP (r = 0.661) and cohort-recorded IUGR (r = 0.335) (Fig. 2E).

*FLT1, ENG, PAPPA2* and *MME* belonged to the blue module, with correlations of 0.927, 0.866, 0.742 and 0.652, respectively, with their assigned module eigengene; *ELMO1* belonged to the pink module. Across 30 subsamples, each containing 80% of the discovery participants, the median best-match Jaccard index for the blue module was 0.867 (range 0.820 – 0.900). Corresponding indices were 0.908, 0.877 and 0.847 when using soft-thresholding powers of 15 and 17 and biweight midcorrelation,

respectively (Fig. 2F; Additional file 1: Fig. S2A – E). These results describe module reconstruction stability conditional on the fixed discovery gene set.

**Associations with maximum antenatal blood pressure**

In the full cohort, clinically adjusted blue-module effects per SD were 7.51 mmHg for SBP (95% CI 3.80 – 11.23) and 4.42 for DBP (2.15 – 6.69; both FDR = 0.00234). Adding lineage proxies yielded 7.02 (2.64 – 11.41) and 4.48 (1.59 – 7.37; both FDR = 0.0338), with module VIF 2.99 (Fig. 3A; Table 2; Fig. S3E).

Excluding blue genes from proxy construction retained the SBP association (6.92 mmHg/SD; 95% CI 2.58 – 11.25; FDR = 0.0418), whereas DBP missed FDR < 0.05 (3.81; 1.11 – 6.51; FDR = 0.0524). The PE-associated eigengene difference decreased from 1.252 SD after clinical adjustment to 0.654 with lineage adjustment and was 0.720 with reconstructed proxies; detailed CIs and FDRs appear in Table S4 (Fig. 3C). Correlations were positive with the extravillous trophoblast proxy ($\rho = 0.577$) and negative with stromal proxy ($\rho = -0.634$; Fig. 3D; Supplementary methods).

Within PE, no SBP or DBP association survived correction. Clinically adjusted FDRs were 0.444 and 0.104. With lineage proxies, effects were 5.95 mmHg/SD for SBP (95% CI 0.58 – 11.31; P = 0.0303) and 4.22 for DBP (0.70 – 7.73; P = 0.0194), both FDR = 0.394. Reconstructed proxies also yielded no corrected association (Fig. 3B, F; Table 2; Fig. S3A – D).

Full-cohort associations survived correction after IUGR adjustment, nonlinear gestational age, or maternal-age/delivery-mode adjustment. Restriction to 28 – 36 weeks (n = 79) yielded no corrected SBP or DBP association (FDR = 0.237 and 0.470; Fig. S3F; Table S2). Outcomes were antenatal maxima.

**External module preservation and score differences between disease groups**

Blue preservation varied across GSE25906, GSE10588 and GSE114691: Zsummary = 3.93, 26.35 and 33.37; medianRank = 11, 2 and 5; measurable genes = 504, 473 and 514 of 543 (Fig. 4A, B, E; Fig. S2F; Table S1). Discovery kME and external score correlations were broadly concordant in the independent cohort (Fig. 4F).

In GSE114691, blue scores increased versus controls in PE (difference 1.159; 95%

CI 0.900–1.419; FDR = $1.74 \times 10^{-9}$), FGR (0.743; 0.466 – 1.020; FDR = $2.68 \times 10^{-5}$) and PE with FGR (1.252; 1.001 – 1.504; FDR = $1.55 \times 10^{-10}$). PE exceeded FGR (0.416; 0.123 – 0.710; FDR = 0.0189), whereas PE with FGR did not clearly differ from PE (0.093; – 0.177 to 0.363; FDR = 0.649; Fig. 4C, D). PE scores also increased in both supportive microarrays (Table S3). Elevation was therefore shared by PE and FGR.

**Cross-cohort consistency and cellular localisation of candidate-gene expression**

The earlier three-cohort random-effects analysis showed directionally consistent, positive PE-associated standardised expression effects for MME, ENG, PAPPA2 and FLT1. Pooled effects were 0.962 SD (95% CI 0.768 – 1.155), 1.064 SD (95% CI 0.816 – 1.312), 1.076 SD (95% CI 0.865 – 1.288) and 1.142 SD (95% CI 0.707 – 1.577), respectively. Heterogeneity differed across these genes, with $I^2$ values of 0%, 32.2%, 0% and 69.8%, respectively. By contrast, ELMO1 showed inconsistent directions across cohorts, and its pooled effect did not meet the statistical threshold (FDR = 0.736; $I^2 = 91.5\%$) (Fig. 5A).

Nine of ten highlighted genes were evaluable in independent RNA-sequencing. MME, FLT1, ENG and PAPPA2 increased in PE ($\log_2$ fold changes 0.660, 3.098, 1.631 and 2.925; genome-wide FDRs 0.00259, $9.47 \times 10^{-12}$, $2.03 \times 10^{-9}$ and $1.29 \times 10^{-9}$). LEP, NDRG1, SERPINE1 and PROCR also increased; ELMO1 decreased ( – 0.262; FDR = 0.0134). KYAT1 was not evaluable under the specified symbol (Fig. 5B; Table 3).

MME expression was higher in isolated PE than in isolated FGR (log2 fold change 0.704; FDR = 0.00977), but no difference was detected between isolated FGR and controls (log2 fold change – 0.045; FDR = 0.866). FLT1, ENG and PAPPA2 were increased not only in PE but also in isolated FGR. None of the nine evaluable candidates survived genome-wide multiple-testing correction in the comparison of PE with FGR versus isolated PE (Table 3; Additional file 1: Fig. S4E). In the discovery cohort, PE-associated expression differences for MME, ENG, PAPPA2 and FLT1 persisted after adjustment for cell-lineage proxies constructed without blue module genes; all FDRs were < 0.001 (Additional file 1: Fig. S4F; Additional file 1: Table

S4).

In the single-cell reference, MME expression was highest in fetal cytotrophoblasts, followed by proliferating cytotrophoblasts and extravillous trophoblasts. Across the major lineages, relative expression of FLT1, ENG and PAPPA2 was highest in extravillous trophoblasts (Fig. 5C; Additional file 1: Fig. S4D). In the supportive laser-capture microdissection data, none of the five evaluable highlighted genes – ENG, FLT1, LEP, MME and NDRG1 – met the within-compartment genome-wide FDR < 0.05 threshold in any of the three compartments (Additional file 1: Fig. S4A, B). Reference-based expression localisation and tissue-compartment comparisons represent different evidence types from independent bulk-tissue RNA-sequencing validation.

**Functional enrichment of the primary module**

Among the 2,239 functional annotation terms tested for the blue module, seven met the within-module FDR < 0.05 threshold. These included negative regulation of DNA-templated transcription (43 overlapping genes; FDR = 0.0201), negative regulation of transcription by RNA polymerase II (34 genes; FDR = 0.0315) and response to endoplasmic reticulum stress (14 genes; FDR = 0.0394) (Fig. 5D).

The HIF-1 signalling pathway contained 12 overlapping genes, but its statistical support depended on the multiple-testing family: FDR was 0.0639 within the blue module and 0.0212 across all tested modules. Cellular response to peptide hormone stimulus did not survive either correction, with within-module and across-module FDRs of 0.305 and 0.195, respectively. Neither vascular smooth muscle contraction nor regulation of vasoconstriction was enriched; FDRs were 1.000 under both corrections (Fig. 5E). The previously retrieved STRING functional association network provided a context for candidate-gene connections (Fig. 5F), not direct evidence of altered vasoconstrictor function.

**Exploratory classification performance of the fixed three-gene score**

The earlier nested feature-selection pipeline achieved a mean AUC of 0.875 across 15 outer fits, with a descriptive SD of 0.061. FLT1 was selected in all 15 fits, whereas ELMO1 and MME were each selected in eight (Fig. 6A, B). The final fixed FLT1–

ELMO1–MME score had an apparent AUC of 0.900 in the discovery cohort (95% bootstrap CI 0.848–0.943). AUCs in the supportive replication cohorts GSE25906 and GSE10588 were 0.763 (95% CI 0.630 – 0.882) and 0.878 (95% CI 0.729 – 0.977), respectively (Additional file 1: Table S5). The nested validation estimates evaluated the entire feature-selection pipeline, not an a priori fixed three-gene panel.

Without refitting coefficients, the score achieved an AUC of 0.986 for isolated PE versus controls in GSE114691 (95% CI 0.957 – 1.000; n = 41) and 0.983 for PE with FGR versus controls (95% CI 0.948 – 1.000; n = 41). The same score had an AUC of 0.820 for isolated FGR versus controls (95% CI 0.675 – 0.950; n = 39) and 0.794 for isolated PE versus isolated FGR (95% CI 0.639 – 0.922; n = 38) (Fig. 6C, D, F).

Post hoc AUC differences versus FLT1 alone were 0.0024 in GSE114691 (95% CI – 0.0095 to 0.0190), 0.0411 in GSE25906 ( – 0.0024 to 0.0928) and – 0.0181 in GSE10588 ( – 0.0543 to 0.0090). FLT1 alone had independent-cohort AUC 0.983. All intervals included zero; incremental discrimination was not established (Fig. 6E; Table S5). These disease-state analyses do not establish perioperative haemodynamic prediction.

## Discussion

### Principal findings

We identified a placental co-expression module associated with PE that contained FLT1, ENG, PAPPA2 and MME and was associated with maximum antenatal blood pressure in the discovery cohort.Full-cohort SBP and DBP associations met the multiplicity-adjusted significance criterion after adjustment for clinical variables and cell-lineage proxies; evidence for SBP was relatively stable when module genes were additionally excluded from proxy construction. Preservation varied across external cohorts, and the fixed score was also elevated in isolated FGR. Taken together, the principal finding is a placental signature supported by cross-cohort expression and network preservation evidence and associated with discovery-cohort blood pressure, rather than an established PE-specific marker of blood pressure severity.

### Shared placental expression signatures and candidate biological leads

Previous studies have identified molecular subtypes of PE and blood pressure-related

transcriptional modules[10, 11]. Building on that work, we combined network stability, external preservation, clinical adjustment and cell-lineage proxies to examine the interpretive scope of these signals. The independent four-group comparison was particularly informative: *FLT1, ENG* and *PAPPA2* were increased in both PE and isolated FGR, and module scores showed a shared pattern. Higher scores in isolated PE than in isolated FGR suggest quantitative differences but do not establish disease specificity. Likewise, failure to detect a difference between PE with FGR and isolated PE does not establish biological equivalence.

Established antiangiogenic mechanisms provide a biological context for the *FLT1* and *ENG* expression findings[7, 8]. Prospective protein studies of PE and FGR nevertheless suggest that adverse maternal angiogenic profiles can arise through different placental protein changes[9]. Our gene-level transcript measurements did not distinguish soluble isoforms, and neither circulating proteins nor endothelial function were measured. We therefore cannot identify circulating mediators responsible for the observed blood pressure associations.

The observed MME expression pattern warrants further investigation. Its expression was higher in PE than in controls and higher in isolated PE than in isolated FGR, whereas no difference was detected between isolated FGR and controls. This pattern remains insufficient to establish PE specificity. Previous work found that extracellular vesicles released from PE placentas carried more active neprilysin[32]. Experimental models reported by He et al. further suggested that excess vesicular neprilysin could impair C-type natriuretic peptide (CNP)–natriuretic peptide receptor B (NPRB)-mediated vasodilation[33]. These independent findings support further investigation of *MME*-related circulating protein levels and enzyme activity. In our healthy reference, *MME* expression was relatively high in cytotrophoblasts, which does not fully agree with the syncytiotrophoblast localisation emphasised in that experimental study. Disease-matched cellular and protein studies are needed to clarify this difference.

Enrichment results surviving within-module correction primarily involved transcriptional regulation and endoplasmic reticulum stress. Support for HIF-1

depended on the correction family, while vascular smooth muscle contraction and regulation of vasoconstriction were not enriched. The module is therefore better described as a placental expression signature associated with stress-related annotations and disease status than as a validated “vasoconstriction module”. Network connections may help generate candidate relationships but cannot establish a causal chain from transcriptional changes to maternal vascular responses.

**Interpretation of blood pressure associations and cell-lineage adjustment**

Attenuation of the PE-associated module difference after lineage adjustment is consistent with the bulk-tissue heterogeneity highlighted by previous cellular-composition studies[12]. We additionally removed direct overlap between module genes and proxy markers. However, the proxies were derived from a healthy term reference and may still reflect both cell abundance and disease-related cell states. Coefficient attenuation does not quantify mediation by cellular composition, and residual associations cannot be interpreted as cell-intrinsic effects.

Full-cohort and within-PE associations address different questions. Although the full-cohort models adjusted for PE status, neither SBP nor DBP associations among the 80 women with PE survived multiple-testing correction. This limits any interpretation of the module as an indicator of variation in blood pressure severity within PE. The primary module was selected using PE status in the same discovery cohort, and blood pressure contributes to disease classification; conditional adjustment cannot remove uncertainty introduced by this selection process. Shared expression shifts between cases and non-cases can also generate gene correlations, meaning that external preservation may partly reflect recurring disease-related or cell-mixture differences. Negative findings in the gestational-age-restricted analysis and in the DBP analysis excluding module genes further show that the evidence was not equally robust across all models.

**Relevance to anaesthetic haemodynamic research**

The link to anaesthesia lies in the hypertension-related biological background of women with PE before they undergo anaesthesia. In specific studies, severe PE was associated with less post-spinal hypotension and lower phenylephrine treatment

requirements[4, 5], while blood pressure, cardiac output and peripheral vascular resistance could follow different patterns[3, 6]. Higher placental module scores therefore cannot be assumed to indicate either greater susceptibility to or protection against hypotension. A testable question is whether measurable circulating correlates of this signature have distinct associations with pre-anaesthetic cardiovascular status and post-anaesthetic pressure and flow responses.

Anaesthetic exposure before tissue collection is another directly relevant consideration. Lekva et al. observed associations of spinal or epidural anaesthesia and other delivery-related variables with placental expression profiles at term[34]. Because that study involved a different gestational-age and disease context, it cannot establish that the specific gene changes observed here were caused by anaesthesia. It nevertheless highlights anaesthesia as an exposure that should be recorded in analyses of tissue collected at delivery. Our datasets lacked information on anaesthetic technique, the interval between drug administration and sampling, and related medications. Adjustment for mode of delivery cannot substitute for adjustment for these factors.

Future validation should obtain pre-anaesthetic maternal blood samples, paired placental tissue and continuous haemodynamic recordings in prospective cohorts. Baseline pressure and flow, the magnitude and sustained burden of post-anaesthetic blood pressure reduction, drug-specific vasopressor requirements and neonatal outcomes should be evaluated separately. Previous anaesthesia trials in PE have examined umbilical arterial acid–base status and uteroplacental vascular resistance as distinct outcomes, underscoring that these should not be combined into a single measure of anaesthetic benefit[35, 36]. Studies should also prospectively record FGR, antihypertensive medication and magnesium sulphate, anaesthetic dose and block level, and the timing of fluid and uterotonic administration, and assess incremental information beyond routine clinical factors. The present placental findings can guide the selection of molecular features for testing, but they do not support recommendations for vasopressor choice or neprilysin-targeted treatment.

**Exploratory classification and the gap to clinical translation**

Although the three-gene score achieved an AUC of 0.986 for PE versus controls in the independent cohort, the paired AUC difference relative to *FLT1* alone was 0.0024, with a 95% CI including zero. Thus, incremental discrimination was not demonstrated. The score also discriminated FGR and should not be described as a PE-specific test. *ELMO1* entered the classification score despite inconsistent directions in expression analyses, illustrating that predictive contribution is not equivalent to a reproducible single-gene association; it also did not belong to the blue module. External evaluation fixed the coefficients but used standardisation across the entire external cohort, so performance remained dependent on cohort composition. Small samples, retrospective comparisons of established disease, and the absence of calibration and decision analyses leave a substantial gap to clinical deployment. Importantly, placental tissue collected at delivery is not available before anaesthesia. Any future blood-based assay requires independent validation and cannot inherit the placental AUC.

**Strengths and limitations**

Strengths include evaluation of the same research question across multiple platforms using sample-level data, a distinction between previously used replication cohorts and a newly introduced external cohort, and reporting of module stability, coverage, cell-lineage sensitivity and findings that did not support the anticipated hypotheses. Inclusion of FGR and combined disease in the independent cohort avoided assessing disease specificity solely through PE–control classification.

The principal limitation is that tissue was obtained at delivery, with no clearly defined temporal alignment or ordering between expression and maximum antenatal blood pressure; causal direction therefore cannot be determined. Blood pressure associations were evaluated only in the discovery cohort and were not replicated using independent blood pressure data. Differences in source diagnoses and gestational age, inclusion of chronic hypertension in the non-PE group, limited medication and labour information, and differences in platform coverage and transcript mapping may all affect interpretation. Network subsampling was conditional on a fixed gene set, and precision was limited for preservation analyses based on 200 permutations and heterogeneity estimates based on only three cohorts. The healthy reference cannot

establish PE-specific cellular changes, and the small compartment analysis with repeated donors yielded no candidate findings surviving multiplicity correction. Without protein, functional or anaesthetic-outcome validation, this remains a molecular association study intended to inform further validation.

## Conclusions

We identified a placental co-expression signature associated with PE, with supporting expression and network-preservation findings across multiple cohorts and an association with maximum antenatal blood pressure in the discovery cohort. The signature also overlapped with FGR, and associations within PE did not survive multiple-testing correction. Candidate genes, including *MME*, warrant further study of potential links among placental expression, circulating molecular measures and haemodynamic phenotypes in obstetric anaesthesia. These findings do not establish a tool for predicting post-anaesthetic hypotension or support individualised vasopressor treatment.

## List of abbreviations

**AUC,** area under the receiver operating characteristic curve; **BH,** Benjamini–Hochberg; **CI,** confidence interval; **CNP,** C-type natriuretic peptide; **CP10K,** counts per 10000; **DBP,** diastolic blood pressure; **FDR,** false discovery rate; **FGR,** fetal growth restriction; **GEO,** Gene Expression Omnibus; **GO,** Gene Ontology; **HC3,** heteroscedasticity-consistent covariance estimator type 3; **IQR,** interquartile range; **IUGR,** intrauterine growth restriction; **KEGG,** Kyoto Encyclopedia of Genes and Genomes; **kME,** module membership; **NPRB,** natriuretic peptide receptor B; **PE,** pre-eclampsia; **ROC,** receiver operating characteristic; **SBP,** systolic blood pressure; **SD,** standard deviation; **sENG,** soluble endoglin; **sFLT1,** soluble fms-like tyrosine kinase 1; **STRING,** protein functional association network database; **TMM,** trimmed mean of M-values; **WGCNA,** weighted gene co-expression network analysis.

## Declarations

### Ethics approval and consent to participate

This study was conducted in accordance with the Declaration of Helsinki. This secondary analysis used only publicly available, de-identified placental transcriptomic data. Under the institutional policy of Yinchuan Maternal and Child Health Hospital Affiliated to Ningxia Medical University, separate ethical approval and renewed informed consent were not required.

## Availability of data and materials

The public datasets analysed in this study are available from the NCBI Gene Expression Omnibus under accessions GSE75010, GSE25906, GSE10588, GSE114691, GSE182381 and GSE93839 . Additional file 1 contains supplementary methods, figures and five focused tables. The source-results and code archive (Additional file 2) contains archived source-result tables, analysis scripts and a guide to their dependencies. Raw sequencing reads are not reproduced in these files.

## Competing interests

The authors declare that they have no competing interests.


## Funding

This study received no specific funding.


## Authors' contributions

Qiang Li, conceived and designed the study, performed the principal data analyses and interpretation, and drafted the manuscript,and critical review and revision of the manuscript; Weiqiang Ma, contributed to data curation, statistical analysis and verification of the results; Yongdong Zhao, contributed to data curation, statistical analysis and verification of the results; Yali Zhang, contributed to methodological review, clinical interpretation and revision of important manuscript content;Haoming Liu, contributed to bioinformatic analyses, visualisation and interpretation of the transcriptomic findings; Mingjun Wang, provided overall supervision and contributed to study design, interpretation of the results, and critical review and revision of the manuscript.


## Acknowledgements

The authors thank the Gene Expression Omnibus (GEO) database and the original

research teams for publicly sharing their data, which made this secondary analysis possible.

# References:

[1]. Dimitriadis, E., et al., Pre-eclampsia. Nat Rev Dis Primers, 2023. 9(1): p. 8.

[2]. Dennis, A.T., A. Xin and M.K. Farber, Perioperative Management of Patients with Preeclampsia: A Comprehensive Review. Anesthesiology, 2025. 142(2): p. 378-402.

[3]. Dyer, R.A., et al., Hemodynamic changes associated with spinal anesthesia for cesarean delivery in severe preeclampsia. Anesthesiology, 2008. 108(5): p. 802-11.

[4]. Aya, A.G.M., et al., Patients with severe preeclampsia experience less hypotension during spinal anesthesia for elective cesarean delivery than healthy parturients: a prospective cohort comparison. Anesth Analg, 2003. 97(3): p. 867-872.

[5]. Hu, L., et al., Comparative Dose-Response Study of Phenylephrine Bolus for the Treatment of the First Episode of Spinal Anesthesia-Induced Hypotension for Cesarean Delivery in Severe Preeclamptic versus Normotensive Parturients. Drug Des Devel Ther, 2022. 16: p. 2189-2198.

[6]. Di Martino, D.D., et al., Maternal hemodynamic profile during pregnancy and in the post-partum in hypertensive disorders of pregnancy and fetal growth restriction. Am J Obstet Gynecol MFM, 2023. 5(3): p. 100841.

[7]. Rana, S., S.D. Burke and S.A. Karumanchi, Imbalances in circulating angiogenic factors in the pathophysiology of preeclampsia and related disorders. Am J Obstet Gynecol, 2022. 226(2S): p. S1019-S1034.

[8]. Margioula-Siarkou, G., et al., The role of endoglin and its soluble form in pathogenesis of preeclampsia. Mol Cell Biochem, 2022. 477(2): p. 479-491.

[9]. Gaccioli, F., et al., Increased Placental sFLT1 (Soluble fms-Like Tyrosine Kinase Receptor-1) Drives the Antiangiogenic Profile of Maternal Serum Preceding Preeclampsia but Not Fetal Growth Restriction. Hypertension, 2023. 80(2): p. 325-334.

[10]. Leavey, K., et al., Unsupervised Placental Gene Expression Profiling Identifies Clinically Relevant Subclasses of Human Preeclampsia. Hypertension, 2016. 68(1): p. 137-47.

[11]. Ackerman, W.E.T., et al., Transcriptomics-Based Subphenotyping of the Human Placenta Enabled by Weighted Correlation Network Analysis in Early-Onset Preeclampsia With and Without Fetal Growth Restriction. Hypertension, 2023. 80(6): p. 1363-1374.

[12]. Campbell, K.A., et al., Placental cell type deconvolution reveals that cell proportions drive preeclampsia gene expression differences. Commun Biol, 2023. 6(1): p. 264.

[13]. Edgar, R., M. Domrachev and A.E. Lash, Gene Expression Omnibus: NCBI gene expression and hybridization array data repository. Nucleic Acids Res, 2002. 30(1): p. 207-10.

[14].Barrett, T., et al., NCBI GEO: archive for functional genomics data sets--update. Nucleic Acids Res, 2013. 41(Database issue): p. D991-5.

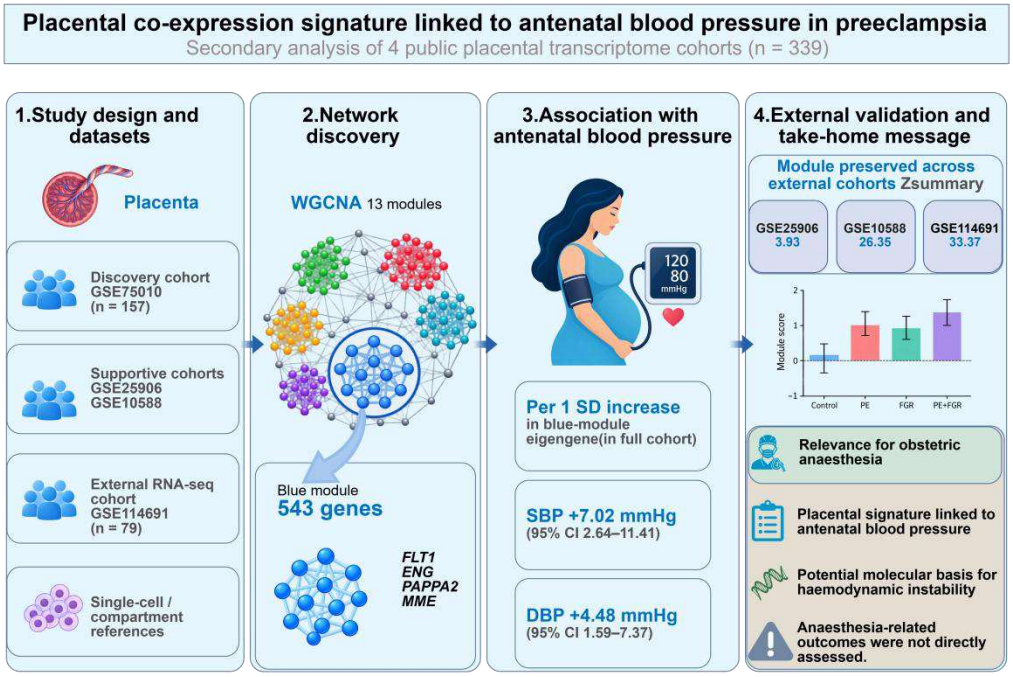
[15]. Tsai, S., et al., Transcriptional profiling of human placentas from pregnancies complicated by preeclampsia reveals disregulation of sialic acid acetylesterase and immune signalling pathways. Placenta, 2011. 32(2): p. 175-82.

[16]. Sitras, V., et al., Differential placental gene expression in severe preeclampsia. Placenta, 2009. 30(5): p. 424-33.

[17]. Awamleh, Z., G.B. Gloor and V.K.M. Han, Placental microRNAs in pregnancies with early onset

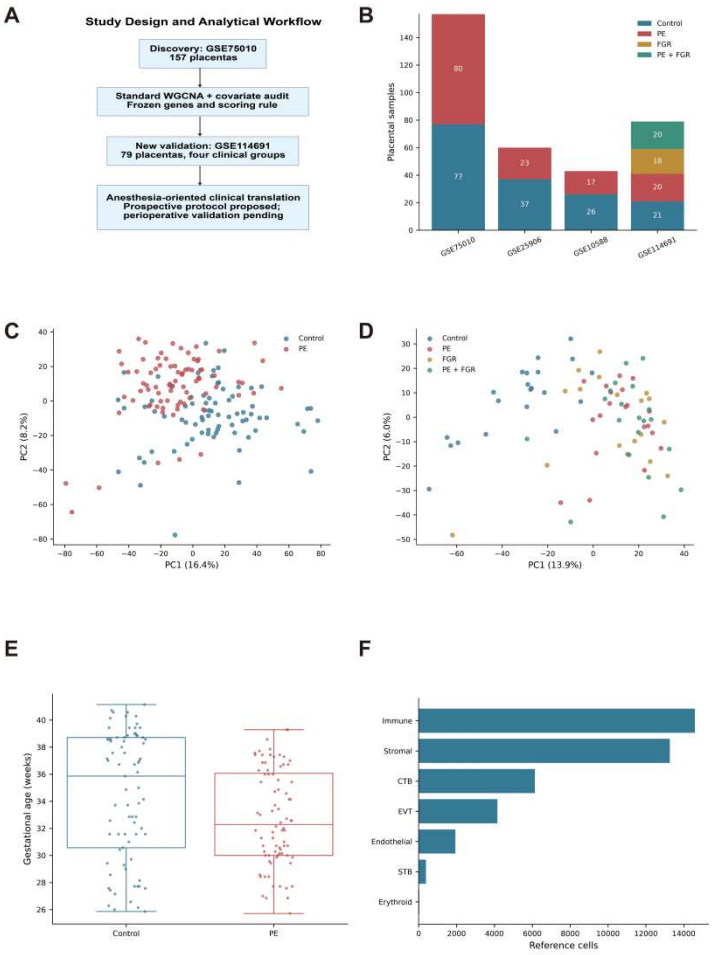
669 intrauterine growth restriction and preeclampsia: potential impact on gene expression and
670 pathophysiology. BMC Med Genomics, 2019. 12(1): p. 91.
671 [18]. Tsang, J.C.H., et al., Integrative single-cell and cell-free plasma RNA transcriptomics elucidates
672 placental cellular dynamics. Proc Natl Acad Sci U S A, 2017. 114(37): p. E7786-E7795.
673 [19]. Pique-Regi, R., et al., Single cell transcriptional signatures of the human placenta in term and
674 preterm parturition. Elife, 2019. 8.
675 [20]. Gormley, M., et al., Preeclampsia: novel insights from global RNA profiling of trophoblast
676 subpopulations. Am J Obstet Gynecol, 2017. 217(2): p. 200.e1-200.e17.
677 [21]. DerSimonian, R. and N. Laird, Meta-analysis in clinical trials. Control Clin Trials, 1986. 7(3): p.
678 177-88.
679 [22]. Robinson, M.D., D.J. McCarthy and G.K. Smyth, edgeR: a Bioconductor package for differential
680 expression analysis of digital gene expression data. Bioinformatics, 2010. 26(1): p. 139-40.
681 [23]. Robinson, M.D. and A. Oshlack, A scaling normalization method for differential expression
682 analysis of RNA-seq data. Genome Biol, 2010. 11(3): p. R25.
683 [24]. Ritchie, M.E., et al., limma powers differential expression analyses for RNA-sequencing and
684 microarray studies. Nucleic Acids Res, 2015. 43(7): p. e47.
685 [25]. Law, C.W., et al., voom: Precision weights unlock linear model analysis tools for RNA-seq read
686 counts. Genome Biol, 2014. 15(2): p. R29.
687 [26]. Langfelder, P. and S. Horvath, WGCNA: an R package for weighted correlation network analysis.
688 BMC Bioinformatics, 2008. 9: p. 559.
689 [27]. Langfelder, P., et al., Is my network module preserved and reproducible? PLoS Comput Biol, 2011.
690 7(1): p. e1001057.
691 [28]. Hayes, A.F. and L. Cai, Using heteroskedasticity-consistent standard error estimators in OLS
692 regression: an introduction and software implementation. Behav Res Methods, 2007. 39(4): p. 709-22.
693 [29]. Szklarczyk, D., et al., The STRING database in 2023: protein-protein association networks and
694 functional enrichment analyses for any sequenced genome of interest. Nucleic Acids Res, 2023. 51(D1):
695 p. D638-D646.
696 [30]. Pedregosa, F., et al., Scikit-learn: Machine Learning in Python. Journal of Machine Learning
697 Research, 2011. 12: p. 2825-2830.
698 [31]. Glickman, M.E., S.R. Rao and M.R. Schultz, False discovery rate control is a recommended
699 alternative to Bonferroni-type adjustments in health studies. J Clin Epidemiol, 2014. 67(8): p. 850-7.
700 [32]. Gill, M., et al., Placental Syncytiotrophoblast-Derived Extracellular Vesicles Carry Active NEP
701 (Neprilysin) and Are Increased in Preeclampsia. Hypertension, 2019. 73(5): p. 1112-1119.
702 [33]. He, C., et al., Excess Neprilysin in Placental EVs Impairs CNP-NPRB-Mediated Vasodilation to
703 Trigger Preeclamptic Hypertension. Circ Res, 2025. 136(12): p. 1526-1541.
704 [34]. Lekva, T., et al., Gene expression in term placentas is regulated more by spinal or epidural
705 anesthesia than by late-onset preeclampsia or gestational diabetes mellitus. Sci Rep, 2016. 6: p. 29715.
706 [35]. Fu, F., et al., A comparison of the effect of phenylephrine and norepinephrine on uteroplacental
707 vascular resistance during the treatment of postspinal hypotension in preeclamptic patients: A
708 randomised controlled study. Eur J Anaesthesiol, 2024. 41(2): p. 150-152.
709 [36]. Higgins, N., et al., The Effect of Prophylactic Phenylephrine and Ephedrine Infusions on Umbilical
710 Artery Blood pH in Women With Preeclampsia Undergoing Cesarean Delivery With Spinal Anesthesia:
711 A Randomized, Double-Blind Trial. Anesth Analg, 2018. 126(6): p. 1999-2006.
712

# Abstract



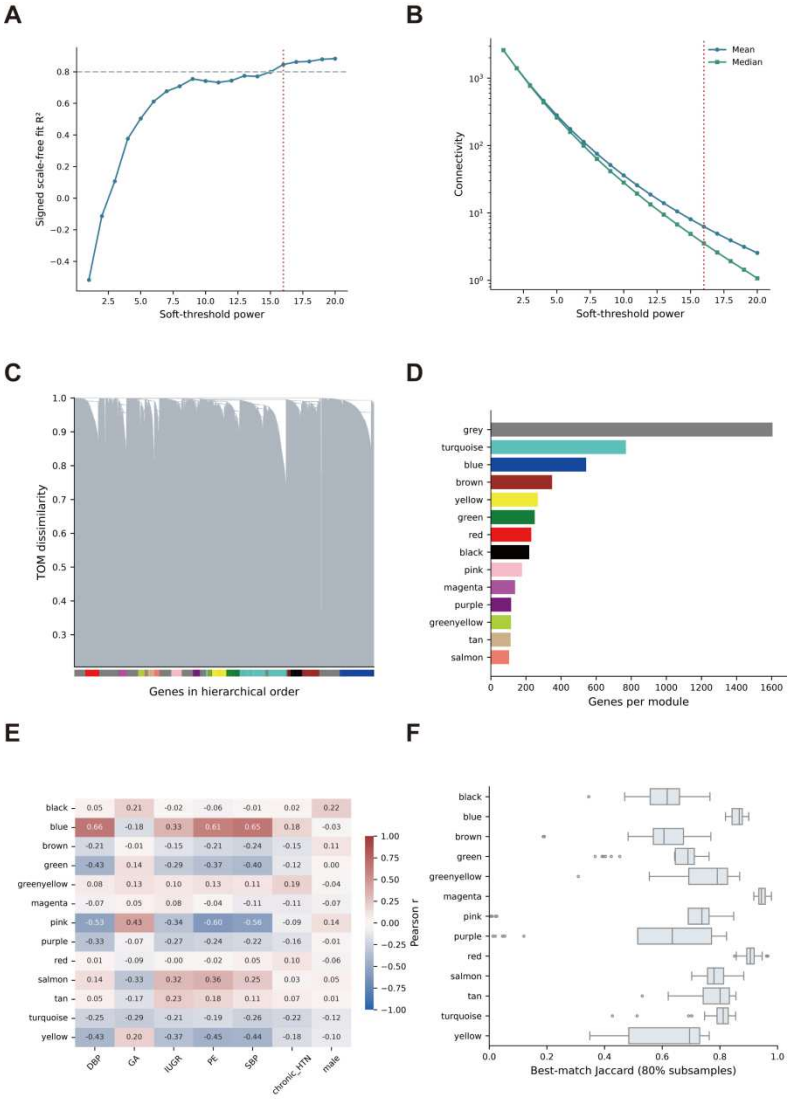

# Figure legends

**Fig. 1 Study workflow, cohort composition and expression overview**




**(A)** Analytical workflow distinguishing completed public-data analyses from a perioperative study plan that has not been implemented. Independent validation expression data were introduced after the discovery network and classification coefficients had been fixed. **(B)** Cohort sizes: GSE75010, 80 PE and 77 non-PE; GSE25906, 23 PE and 37 controls; GSE10588, 17 PE and 26 controls; GSE114691, 20 PE, 21 controls, 18 FGR and 20 PE with FGR. **(C, D)** Principal component analyses of the 5000 most variable genes in GSE75010 and GSE114691, respectively. Genes were standardised within each cohort; axes indicate the proportion of variance explained. No samples were excluded on the basis of disease separation in these plots. **(E)** Gestational-age distributions by PE status in the discovery cohort (n = 157). **(F)** Cell counts after grouping 40494 individually profiled reference cells into seven major lineages. Counts reflect the sampling composition of the reference, not cell proportions in the bulk-tissue cohorts. All panels are descriptive; no inferential P values are provided.

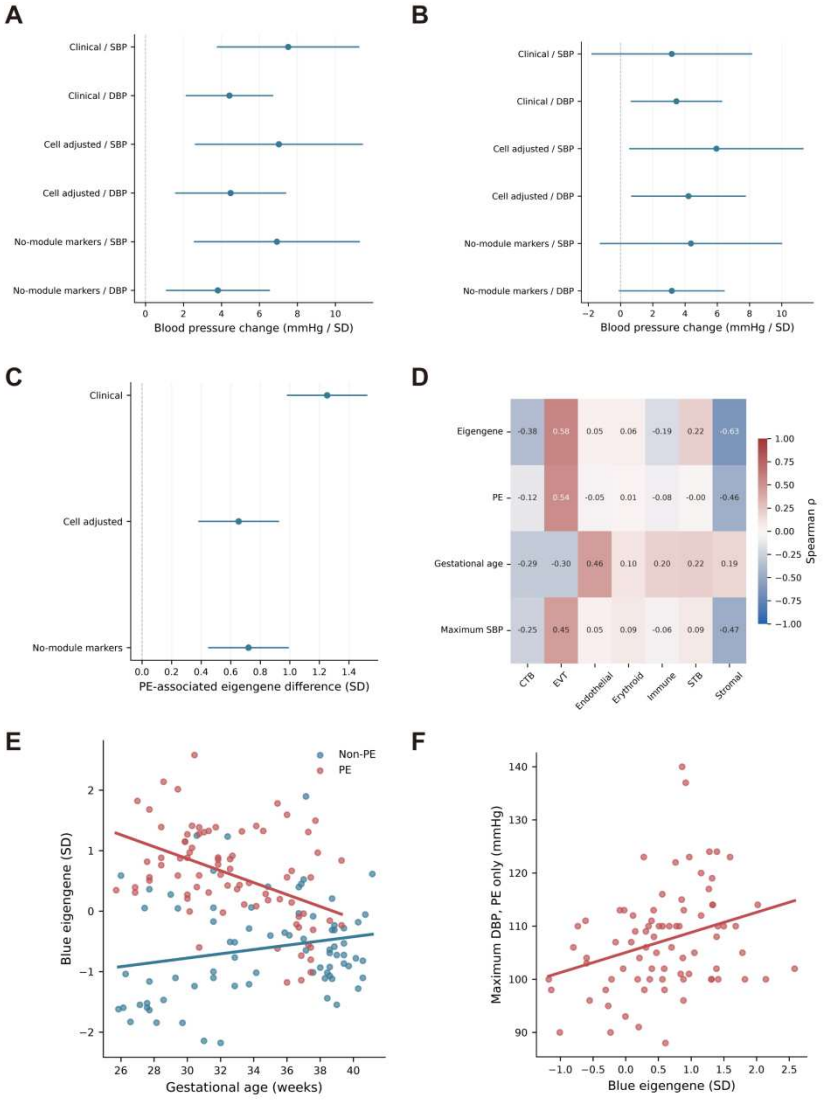
**Fig. 2 Signed WGCNA network and internal stability**




**(A)** Signed scale-free topology fit across soft-thresholding powers 1–20. The horizontal dashed line indicates 0.80; the vertical line marks the selected power of 16. **(B)** Mean and median connectivity on a logarithmic scale. Network sparsity was also considered during power selection. **(C)** Hierarchical clustering dendrogram of 5000 genes based on signed topological overlap, with module colours below. The vertical axis shows the range containing the actual merge heights. **(D)** Gene counts for each assigned module and the grey unassigned set. **(E)** Correlations between 13 assigned module eigengenes and clinical traits; colours and values represent Pearson's r. Complete P values and 91-test correction results are provided in the source-results and code archive (module_trait_correlations.csv). **(F)** Best-match Jaccard indices after network reconstruction in 30 subsamples, each comprising 80% of participants, with

parameters and the 5000-gene set fixed. Network construction included 157 participants, and each subsample included 125. Subsampling statistics describe module reconstruction stability, not confidence intervals for biological effects.

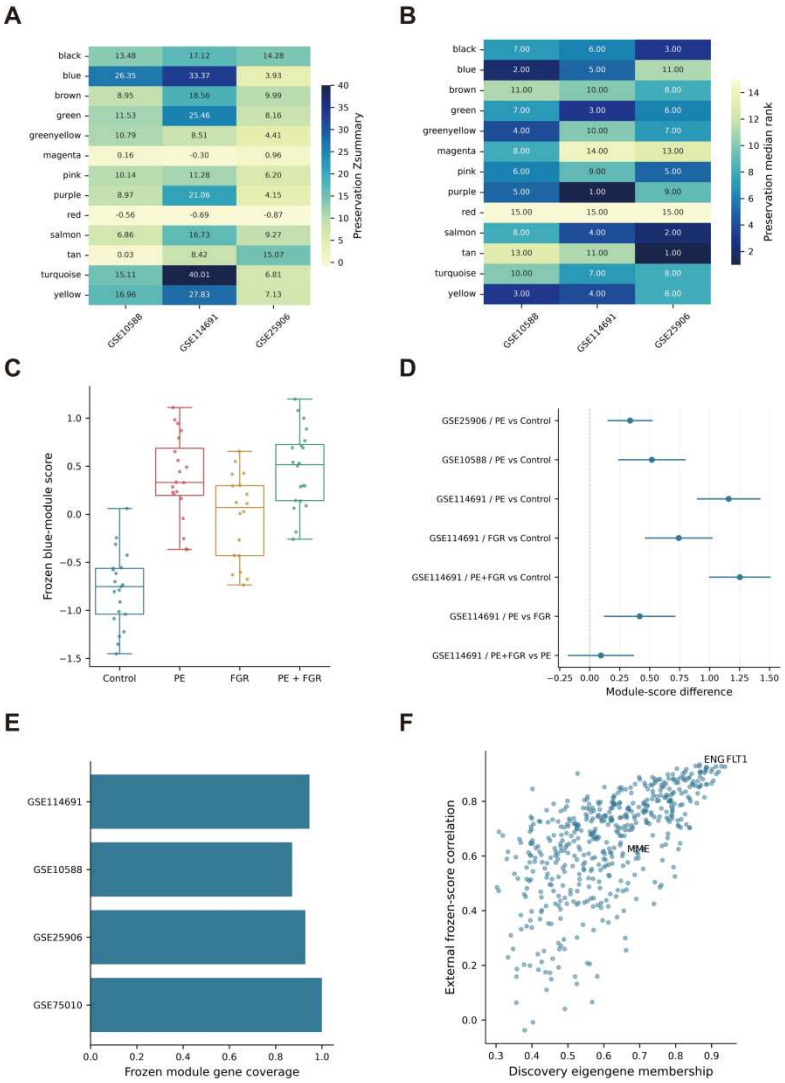
**Fig. 3 Covariate adjustment and within-PE blood pressure associations**




**(A, B)** Primary module blood pressure associations in all 157 participants and within 80 women with PE, respectively. Points show mmHg differences per discovery-cohort SD increase in the module eigengene; horizontal lines show 95% CIs based on HC3 robust variance and the t-distribution. Clinical adjustment included gestational age, fetal sex and chronic hypertension, with additional adjustment for PE diagnosis in full-cohort models. Cell-adjusted models added six reference-derived lineage principal components. Models excluding module markers added seven reconstructed components after removing all 543 blue module genes. Covariates constant within a

761 subset were omitted. Within each model and population, FDR correction covered 13
762 modules × 2 blood pressure outcomes, not only the displayed module. **(C)**
763 PE-associated standardised module eigengene differences and robust 95% CIs under
764 three adjustment schemes (n = 157). **(D)** Spearman correlations of seven lineage
765 proxy scores with the module eigengene, PE diagnosis, gestational age and maximum
766 SBP. Proxy scores are not deconvolved cell proportions. **(E)** Gestational age and
767 module eigengene by group. **(F)** Maximum antenatal DBP and module eigengene
768 among women with PE. Fitted lines in E and F are unadjusted descriptive least
769 squares fits; adjusted inference is based on A, B and the complete model tables
770 (Additional file 1: Table S2). None of the outcomes represents intraoperative blood
771 pressure.

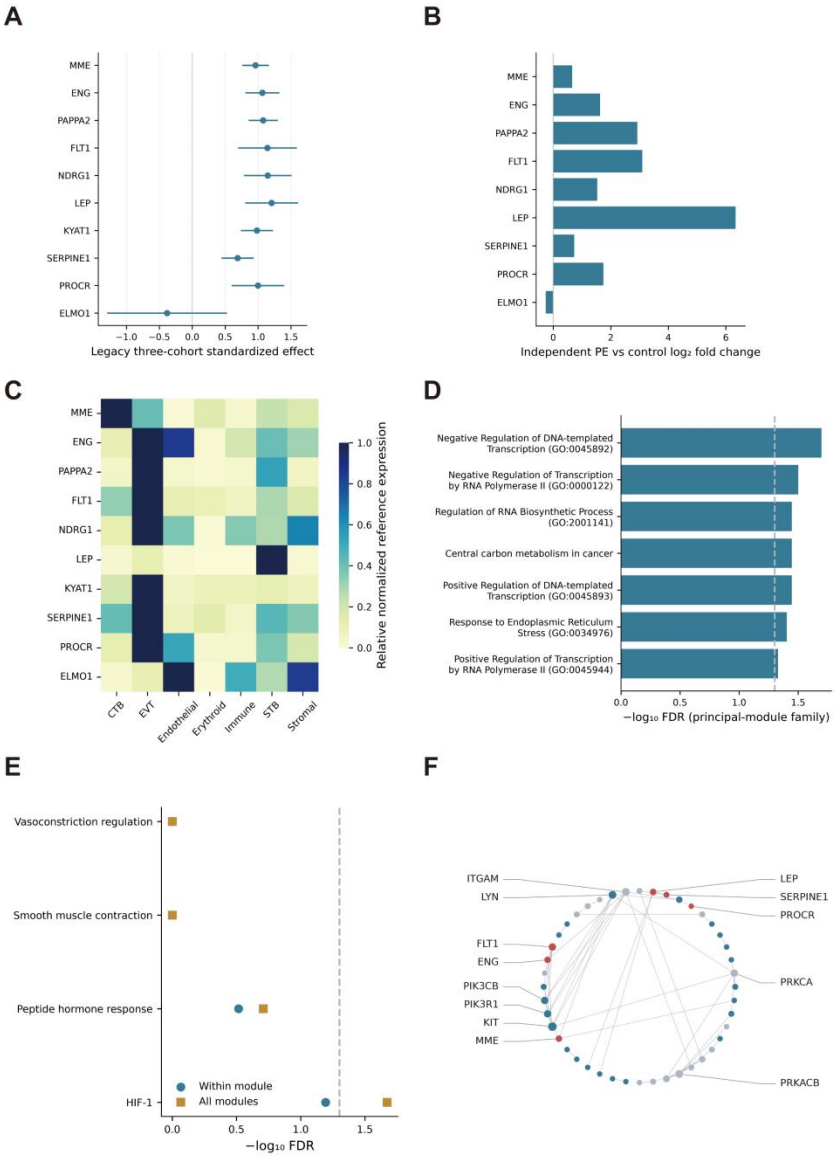
772 **Fig. 4 External network preservation and score comparisons across disease**
773 **groups**




**(A, B)** WGCNA Zsummary and medianRank for all assigned modules in GSE25906, GSE10588 and GSE114691, using shared measurable genes and 200 permutations per cohort. Higher Zsummary and lower medianRank indicate relatively stronger preservation. Zsummary depends on module size; medianRank provides rankings that are less size-dependent. Neither statistic tests differential expression or causality. **(C)** Fixed blue module scores in the independent cohort: 21 controls, 20 PE, 18 FGR and 20 PE with FGR. Scores are the mean within-cohort standardised expression of available fixed genes multiplied by the signs of their discovery-cohort membership. **(D)** Welch mean differences and 95% CIs for the two previously analysed replication cohorts and the five prespecified comparisons in the independent cohort. FDR families include all assigned modules and comparisons within each cohort. **(E)** Fixed-gene coverage in the discovery cohort, GSE25906, GSE10588 and GSE114691:

543/543, 504/543, 473/543 and 514/543, respectively. **(F)** Discovery-cohort membership versus correlation with the external fixed score for 514 evaluable blue module genes. This is a descriptive comparison of connectivity patterns, not an independent gene-wise significance screen; the evaluated genes also contribute to the score.

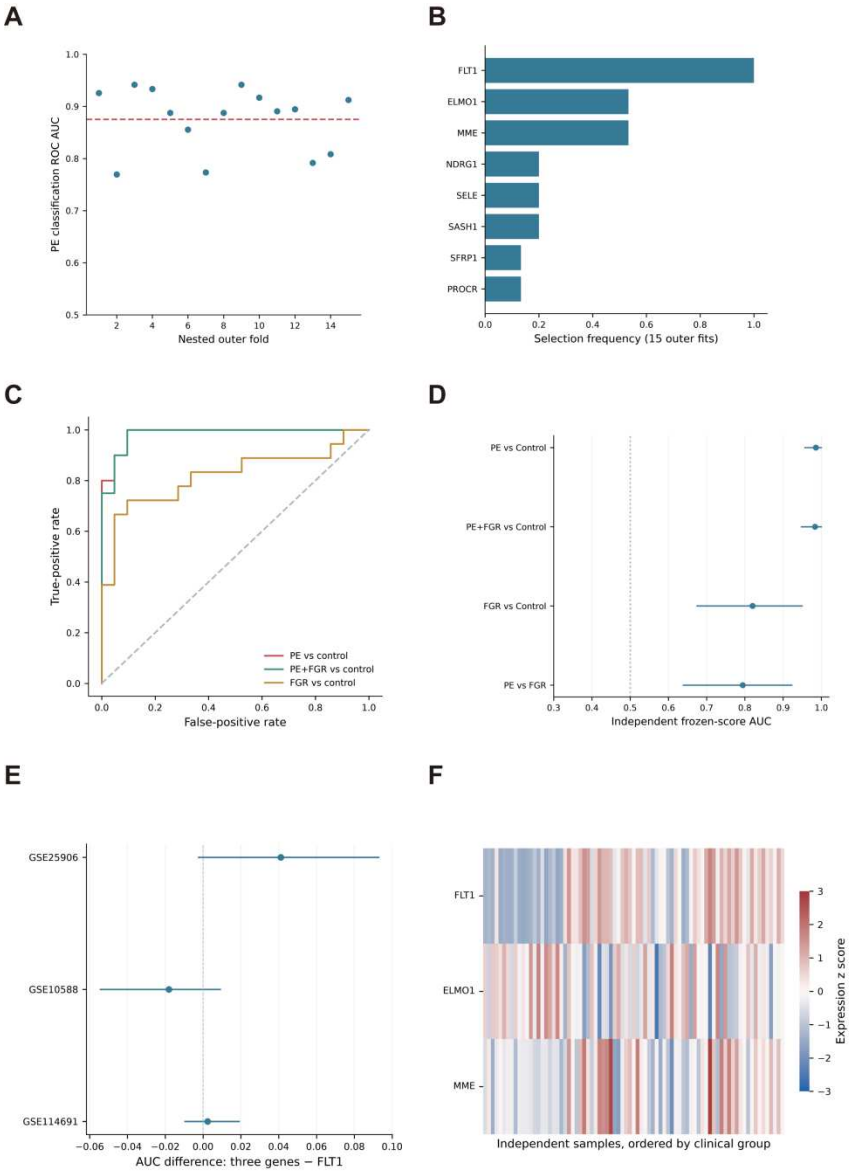
**Fig. 5 Candidate-gene expression, cellular reference localisation and functional enrichment**




**(A)** Random-effects pooled standardised PE expression effects and normal-approximation 95% CIs for ten candidates across three previously analysed cohorts. Units are expression SDs, not $\log_2$ fold changes; heterogeneity estimates from few cohorts remain uncertain. **(B)** limma–voom $\log_2$ fold changes for 20 PE versus 21

controls in independent GSE114691, showing evaluable candidates only. Bar lengths do not indicate significance; genome-wide FDRs are in Table 3 and the source-results and code archive. **(C)** Reference expression aggregated by major lineage after cell-library normalisation. For relative localisation, log(1 + mean CP10K) was divided by each gene's maximum; colours cannot compare absolute expression across genes. This is healthy-reference localisation, not disease differential expression. **(D)** Seven terms with the lowest within-blue-module FDR, selected from the complete test family, including zero-overlap terms. The reference line denotes FDR = 0.05; testing was not restricted to displayed terms. **(E)** Within-module and across-module correction for prespecified pathways. HIF-1 support depends on the correction family; peptide hormone response, smooth muscle contraction and regulation of vasoconstriction lacked multiplicity-adjusted support. A larger across-module family does not necessarily yield larger BH-adjusted values because the overall P-value distribution also changes. **(F)** Previously retrieved high-confidence STRING functional association network. Red nodes are named candidates, blue nodes are other members of the current blue module, and grey nodes are other queried genes; node area increases with connectivity. Edges are not experimentally confirmed physical interactions, and this is not the complete interaction network of the newly constructed module.

**Fig. 6 Fixed classification score performance and incremental discrimination**




**(A)** ROC AUCs from 15 outer fits of the earlier nested feature-selection pipeline, using five folds and three repeats. The horizontal line denotes the mean; dependent folds are not independent inferential replicates. **(B)** Eight features with the highest selection frequencies. Feature filtering and fitting were performed within training folds. **(C)** ROC curves for the fixed FLT1–ELMO1–MME score discriminating PE, PE with FGR and FGR from controls in the independent cohort, without coefficient refitting. **(D)** Independent-cohort AUCs and 95% CIs from 2000 stratified bootstrap resamples, additionally including PE versus FGR; sample sizes were 41, 41, 39 and 38, respectively. **(E)** AUC differences between the three-gene score and FLT1 alone in three external cohorts, from a post hoc comparison added after the main score

evaluation. Horizontal lines show 95% intervals from 2000 paired stratified bootstrap resamples; positive values favour the three-gene score. No retuning was performed, and incremental benefit was not established. **(F)** Within-cohort standardised three-gene expression in 79 independent samples, ordered as controls, PE, FGR and PE with FGR. External standardisation used the entire external cohort without outcome labels but remained cohort-adaptive, rather than directly deployable for a single new patient. Outcomes represent established placental disease states, not future PE, anaesthesia-related hypotension or vasopressor responses.

## Tables

**Table 1 Study datasets and their analytical roles**

| Dataset | Role and assay | Observational units | Group composition | Interpretive information |
|---|---|---|---|---|
| GSE75010 | Discovery; microarray | 157 bulk samples | PE 80; non-PE 77 | Individual gestational age and maximum antenatal blood pressure available. |
| GSE25906 | Supportive replication; microarray | 60 bulk samples | PE 23; controls 37 | Previously used in exploratory analyses. |
| GSE10588 | Supportive replication; microarray | 43 bulk samples | PE 17; controls 26 | Previously used; clinical covariate availability limited. |
| GSE114691 | New external evaluation; RNA sequencing | 79 bulk samples | Controls 21; PE 20; FGR 18; PE + FGR 20 | No individual gestational age, blood pressure or anaesthetic outcomes in the supplied clinical annotation. |
| GSE182381 | Cellular reference; single-cell RNA sequencing | 40494 reference cells | 27 clusters; 7 major lineages | Healthy term reference. Cells are not independent patients. |
| GSE93839 | Compartment context; laser-capture microarray | 23 compartment samples | Invasive 3/4; endovascular 4/4; syncytial 4/4 (PE/control) | Repeated compartments from donors; not 23 independent patients. |

**PE,** pre-eclampsia; **FGR,** fetal growth restriction; **PE + FGR,** coexistence of both conditions. The first four bulk-tissue cohorts comprise 339 samples; single-cell and laser-capture microdissected compartment data are excluded from this total. The 77 non-PE controls in GSE75010 include 24 women with chronic hypertension. Numerators and denominators in compartment composition indicate PE and control sample counts, respectively, not incidence proportions.

**Table 2 Associations of the blue module with maximum antenatal blood pressure**

| Population | Model | Outcome | n | β (95% CI), mmHg | P | FDR |
|---|---|---|---|---|---|---|
| Full cohort | M1 | SBP | 157 | 7.51 (3.80, 11.23) | 0.000101 | 0.00234 |
| Full cohort | M1 | DBP | 157 | 4.42 (2.15, 6.69) | 0.00018 | 0.00234 |
| Full cohort | M2 | SBP | 157 | 7.02 (2.64, 11.41) | 0.00188 | 0.0338 |
| Full cohort | M2 | DBP | 157 | 4.48 (1.59, 7.37) | 0.0026 | 0.0338 |
| Full cohort | M3 | SBP | 157 | 6.92 (2.58, 11.25) | 0.00196 | 0.0418 |
| Full cohort | M3 | DBP | 157 | 3.81 (1.11, 6.51) | 0.00605 | 0.0524 |
| Within PE | M1 | SBP | 80 | 3.18 (−1.77, 8.12) | 0.205 | 0.444 |
| Within PE | M1 | DBP | 80 | 3.46 (0.66, 6.26) | 0.016 | 0.104 |
| Within PE | M2 | SBP | 80 | 5.95 (0.58, 11.31) | 0.0303 | 0.394 |
| Within PE | M2 | DBP | 80 | 4.22 (0.70, 7.73) | 0.0194 | 0.394 |
| Within PE | M3 | SBP | 80 | 4.37 (−1.25, 9.98) | 0.125 | 0.407 |
| Within PE | M3 | DBP | 80 | 3.17 (−0.07, 6.41) | 0.0547 | 0.39 |

Effects are mmHg differences per one discovery-cohort SD increase in the module eigengene. M1 adjusts for gestational age, fetal sex and chronic hypertension, with additional PE-status adjustment in the full cohort. M2 adds six cell-lineage proxy principal components to M1. M3 adds seven lineage principal components reconstructed after excluding all 543 blue module genes. All proxy marker sets exclude the named candidate genes. CIs use HC3 robust variance and the t-distribution and are nominal 95% intervals without multiplicity correction. Two-sided P values are BH-corrected across 13 modules × 2 outcomes within each model and population. All blood pressures are antenatal maxima. All 32 primary-module rows appear in Additional file 1: Table S2; the complete 416-row family is retained in S5_All_BP_models.csv in Additional file 2.

**Table 3 Candidate-gene expression comparisons in the independent RNA-sequencing cohort**

## A.Disease groups versus controls

| Gene | PE vs controls | FGR vs controls | PE + FGR vs controls |
|---|---|---|---|
| MME | 0.660 (0.00259) | −0.045 (0.866) | 0.697 (0.0013) |
| FLT1 | 3.098 ($9.47 \times 10^{-12}$) | 1.744 ($4.52 \times 10^{-6}$) | 3.136 ($2.01 \times 10^{-12}$) |
| ENG | 1.631 ($2.03 \times 10^{-9}$) | 1.018 ($3.19 \times 10^{-5}$) | 1.891 ($1.79 \times 10^{-11}$) |
| PAPPA2 | 2.925 ($1.29 \times 10^{-9}$) | 1.924 ($7.96 \times 10^{-6}$) | 2.734 ($1.83 \times 10^{-9}$) |
| ELMO1 | −0.262 (0.0134) | −0.151 (0.173) | −0.216 (0.0427) |
| LEP | 6.339 ($1.21 \times 10^{-10}$) | 3.989 ($1.94 \times 10^{-6}$) | 6.299 ($8.48 \times 10^{-11}$) |
| NDRG1 | 1.530 ($3.3 \times 10^{-8}$) | 0.801 (0.00117) | 1.548 ($9.59 \times 10^{-9}$) |
| SERPINE1 | 0.729 (0.00118) | 0.760 (0.000954) | 1.062 ($4.86 \times 10^{-6}$) |
| PROCR | 1.745 ($2.22 \times 10^{-9}$) | 1.324 ($2.76 \times 10^{-6}$) | 1.932 ($8.48 \times 10^{-11}$) |
| KYAT1 | NA | NA | NA |

## B.Comparisons between disease groups

| Gene | PE vs controls | FGR vs controls |
|---|---|---|
| MME | 0.704 (0.00977) | 0.037 (1.000) |
| FLT1 | 1.354 (0.0072) | 0.038 (1.000) |
| ENG | 0.612 (0.0478) | 0.260 (1.000) |
| PAPPA2 | 1.002 (0.0782) | −0.192 (1.000) |
| ELMO1 | −0.111 (0.473) | 0.046 (1.000) |
| LEP | 2.349 (0.0265) | −0.040 (1.000) |
| NDRG1 | 0.728 (0.0224) | 0.018 (1.000) |
| SERPINE1 | −0.030 (0.946) | 0.332 (1.000) |
| PROCR | 0.421 (0.231) | 0.188 (1.000) |
| KYAT1 | NA | NA |

Cells show $\log^2$ fold change (genome-wide FDR); positive values indicate higher

expression in the first-named group. Sample sizes: controls, 21; PE, 20; FGR, 18; PE + FGR, 20. Each limma–voom comparison applies BH correction to two-sided P values across all 26044 tested genes, not only the displayed candidates. NA indicates that the specified gene symbol was not evaluable, not a zero effect. Unrounded effects, raw P values and FDRs are retained in Table3_Independent_genes.csv in the source-results and code archive (Tables/Table3_Independent_genes.csv).

## Supplementary Files

This is a list of supplementary files associated with this preprint. Click to download.

- AdditionalfileFigureLegendsMethodsandTables2026.10.08.docx